PERGAMON

Microelectronics Reliability 41 (2001) 847–854

MICROELECTRONICS RELIABILITY

www.elsevier.com/locate/microrel

High injection effects on noise characteristics of Si BJTs and SiGe HBTs

M.J. Martín-Martínez *, S. Pérez, D. Pardo, T. González

Departamento de Física Aplicada, Ayundanrte de Facultad, Universidad de Salamanca, Plaza de la Merced s/n., 37008 Salamanca, Spain

Received 26 December 2000; received in revised form 9 February 2001

Abstract

We present a physically based comparison of the current spectral densities in a SiGe heterojunction bipolar transistors (HBT) and a Si bipolar junction transistor (BJT) of identical geometry and doping levels, based on the direct evaluation of emitter, base and collector current fluctuations. An ensemble Monte Carlo (EMC) simulator self-consistently coupled with a 2D Poisson solver has been employed for the calculations. In the studied bias range, the largest reduction of the RF current noise values in the HBT as compared with the BJT derives from the spectral density of base current fluctuations, S_{J_B}, and from the spectra of the cross-correlation between emitter and base current fluctuations, $S_{J_B J_E}$. This is due to the fact that the base current in the HBT is strongly reduced as a consequence of the lower gap of the SiGe base. At low injection, the collector spectral density S_{J_C} exhibits a typical shot noise response while S_{J_B} is governed by thermal noise. At high injection, the presence of hot carriers in the base–collector junction (which are less important in the HBT than in the BJT due to the SiGe/Si hetero-interface), the high carrier concentration in the base and the base push-out provokes the deviation of S_{J_C} from the pure shot behavior. Under these conditions, the S_{J_B} term can be neglected in the total noise analysis of the HBT for lower values of J_C, than in the BJT due to the Ge content benefits.

1. Introduction

As a result of the possibilities offered by the band-gap engineering, SiGe heterojunction bipolar transistors (HBTs) offer extremely high values of common-emitter DC-current gain (β) and transition frequency (f_T) [1] together with excellent broad-band noise characteristics [2] which make these devices powerful for modern communication systems. For this reason, the study of high-frequency noise in HBTs constitutes an important feature for the development of these devices. Moreover, transistor high-frequency noise becomes a crucial aspect in communication systems, for example it sets the signal-to-noise level at the input of the low-noise amplifier. Due to the fact that the optimization of low-noise devices through fabrication can be very expensive and time consuming, an adequate modeling of transport based on a microscopic model is essential to characterize and improve high speed and low-noise SiGe HBT technology. The EMC method provides accurate static results (mean velocity, current, etc.) under non-equilibrium carrier-lattice conditions (as occurs in a sub-micrometer base) [3] and affords direct calculation of fluctuations in these magnitudes.

In high-speed integrated circuits HBTs operate in the normal active mode, and are typically biased at high current densities (even in quasi-saturation) to achieve the largest values of f_T. Therefore, high-injection phenomena may occur in the transistor and cause severe degradation in key transistor parameters such as β, transconductance (g_m) and f_T. Consequently the high-injection effects can be relevant in the noise performance of the devices and have to be studied carefully.

In this work we present the first physically based determination of spectral densities in a real HBT as compared with an identical bipolar junction transistor

* Corresponding author. Tel.: +34-923-294436; fax: +34-923-294584.

E-mail address: mjmm@gugu.usal.es (M.J. Martín-Martínez).

0026-2714/01/$ - see front matter
PII: S0026-2714(01)00022-1

(BJT), based on the direct evaluation of emitter, base and collector current fluctuations by means of a EMC simulator. This method allows one to gain a microscopic understanding of the different noise sources without additional assumptions about the origin of fluctuations [4]. We shall relate the noise sources to the internal mechanisms that control the transport in the devices (band discontinuities, injection level, presence of hot carriers, etc.), [5,6] paying special attention to the different bias conditions in the active mode.

The paper is organized in the following manner. The geometry and doping profiles of the simulated Si BJT and SiGe HBT together with several details related to the 2D EMC simulator used for the calculations are presented in Section 2. In Section 3 we report the results of the comparison between the BJT and the HBT for both DC and noise performance. High-injection effects on the DC performance when operating at high bias conditions are described in Section 3.1. In Section 3.2 the main features of the frequency dependence of the current spectral densities are reported. Based on the observations of the previous sections, in Section 3.3 the bias dependence of the RF base and collector spectral densities is explained, paying special attention to the different regimes of device operation. Finally, Section 4 summarizes the main conclusions of our work.

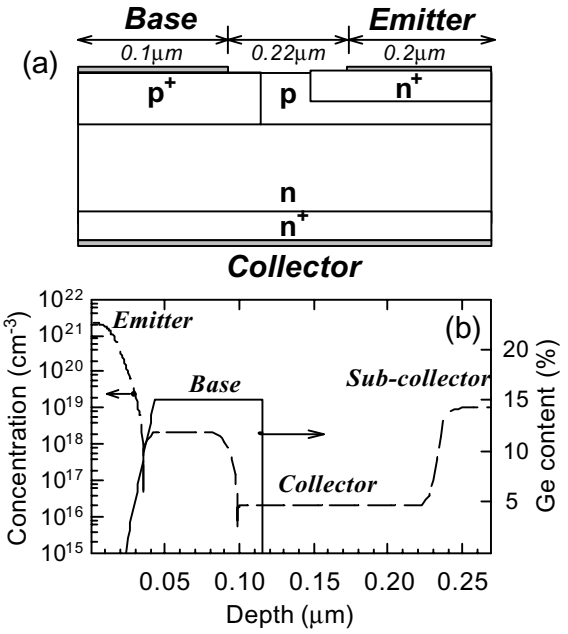

Fig. 1. (a) Geometry of the BJT and HBT. (b) Doping and HBT Ge vertical profiles.

2. Simulated devices and transport model

A detailed study of a Si BJT and a Si-emitter/SiGe-base/Si-collector HBT with identical geometry (Fig. 1(a)) in common-emitter configuration is reported. For realizing a clear comparison, both structures have a similar vertical doping and the HBT has a similar Ge profile to those of the devices analyzed in Ref. [6] (Fig. 1(b)). The Ge percentage in the HBT has a trapezoidal shape which varies linearly from 0% to 15% Ge in 0.025 μm. The total Ge effective thickness is 0.09 μm. The Si/SiGe heterojunction is located within the collector region at a distance of 15 nm from the base. For the calculations we use a 2D EMC simulator that is an extension of a previous 1D version already proved to be a successful tool for bipolar noise studies [4,5]. The microscopic model implemented in the simulator enables one to follow the electron and hole dynamics simultaneously. In the base of the HBT we simulate a SiGe layer grown on a [0 0 1] Si substrate under biaxial compressive strain [4]. The scattering mechanisms considered for electrons and holes are described in Ref. [4].

A variable rectangular mesh (vertical cells ranging from 10 to 25 Å and horizontal cells of 50 Å) locally depending on the doping is used to solve the Poisson equation at time steps of 2.5 fs. To deal with the highly doped regions existing in realistic devices, our simulator includes effects such as band-gap narrowing, impurity deionization and the Pauli exclusion principle. In order to reduce the computation time, the simulated doping level of the emitter layer takes a value of 3×10^{19} cm^{-3}, lower than the real value of 2×10^{21} cm^{-3} reported in Fig. 1(b). This lower doping involves no significant change in the results, since this layer is an ohmic region playing no essential role in the device behavior, which is fundamentally controlled by the p-base and the n-collector region.

The accurate calculation of the instantaneous bipolar current flowing through each electrode by means of a multiparticle Monte Carlo simulation is not straightforward due to the complex 2D geometry of BJTs and HBTs. As the purpose of our work is the investigation of the noise characteristics throughout the evaluation of the instantaneous current fluctuations taking place in the devices, an accurate determination of the instantaneous bipolar current flowing at each electrode is necessary. To this purpose, a technique based on the Ramo–Shockley (RS) theorem similar to that used in Ref. [7] was followed for the calculation of the instantaneous emitter, base and collector electrodes. This theorem can be applied for bipolar structures and is valid for an inhomogeneous dielectric medium under time-varying potentials of the electrodes, which makes it useful for application in realistic BJTs and HBTs.

Once the electrode current densities are extracted during a total time $T = n\mathrm{d}t$ divided into n time steps of duration $\mathrm{d}t$, we handle them to analyze and compare the

noise behaviors of the BJT and of the HBT. The mathematical quantities that characterize the current noise behavior of these devices are: the autocorrelation functions of the emitter, base and collector current fluctuations, $C_{J_E}(t)$, $C_{J_B}(t)$, $C_{J_C}(t)$, respectively, and the terms arising from the cross-correlation between pairs of these quantities. For instance, the autocorrelation function of current fluctuations of the i (emitter, base or collector) electrode can be calculated from the recorded (at each time step $m\,\mathrm{d}t$ where the index m varies from 0 to n) discrete values of the current densities and expressed by:

$$C_{J_i}(l\,\mathrm{d}t) = \frac{1}{n-k}\sum_{m=k+1}^{n} \delta J_i((m-l)\mathrm{d}t)\delta J_i(m\,\mathrm{d}t) \tag{1}$$

where the index l varies from 0 to k, assuming that the autocorrelation function takes zero value for times longer than $k\,\mathrm{d}t$ and $\delta J_i(t) = J_i(t) - \overline{J_i}$ (the upper bar indicates time average). The cross-correlation function of the electrode i and the electrode j current fluctuations is given by:

$$C_{J_iJ_j}(l\,\mathrm{d}t) = \frac{1}{n-k}\sum_{m=k+1}^{n} \delta J_i((m-l)\mathrm{d}t)\delta J_j(m\,\mathrm{d}t) \tag{2}$$

where the index l varies from $-k$ to k, assuming that the cross-correlation function takes zero value for times $l\,\mathrm{d}t < -k\,\mathrm{d}t$ and $l\,\mathrm{d}t > k\,\mathrm{d}t$.

The current spectral densities characterize the noise over a given frequency range and are obtained by Fourier transforming the autocorrelation functions. The spectral densities of an electrode i current fluctuations (S_{J_i}) and the cross-correlation spectra of pairs (i and j) of these quantities ($S_{J_iJ_j}$), can be expressed in discrete form by:

$$S_{J_i}(f) = 4\,\mathrm{d}t\sum_{l=0}^{k} C_{J_i}(l\,\mathrm{d}t)\cos(2\pi f l\,\mathrm{d}t) \tag{3}$$

$$S_{J_iJ_j}(f) = 2\,\mathrm{d}t\sum_{l=-k}^{k} C_{J_iJ_j}(l\,\mathrm{d}t)\exp(j2\pi f l\,\mathrm{d}t) \tag{4}$$

3. Results

3.1. DC analysis

The base, J_B, and collector, J_C, current densities in the BJT and HBT are shown in Fig. 2(a) as a function of V_{BE}, for V_{CB} equal to 1.0 V. We show current values in the range of V_{BE} where these devices are typically biased. The currents in the simulated devices show an analogous behavior to that found experimentally in similar structures [6]. At low-bias conditions, J_B and J_C (except in the HBT) increase exponentially with V_{BE}. The $J_{C,HBT}/J_{C,BJT}$ ratio shows the "heterojunction effect" originated by the reduction in barrier height for electron injection from the Si-emitter to the SiGe-base of the HBT as compared to that of the BJT (Fig. 2(b)). Also, the more effective confinement of holes in the base of the HBT slightly reduces the flow of holes injected into the emitter or $J_{B,HBT}$. In the trapezoidal Ge HBT a decrease in the slope of J_C with increasing V_{BE} is observed (*Ge-ramp effect*) instead of the typical slope of 60 mV per decade (at room temperature) found in the Si BJT. This is due to the fact that the movement of the edge of the space charge region (SCR) in the base has an effect on J_C [8]. Thus, in this range, a bias-independent constant current gain, β, is found in the BJT, while, being significantly higher, β decreases with J_C in the HBT (Fig. 2(c)).

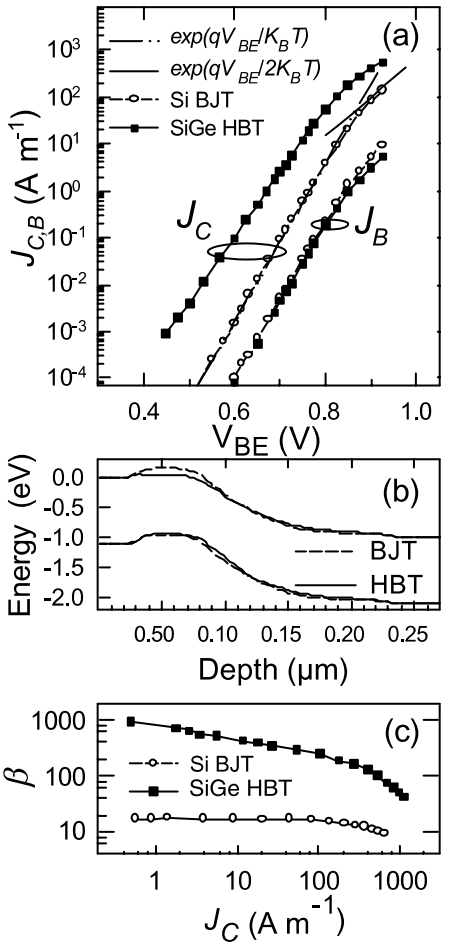

Fig. 2. (a) Simulated base- and collector-current densities (J_B and J_C) as a function of V_{BE} for $V_{CB} = 1.0$ V in the Si BJT and SiGe HBT. (b) Valence and conduction band diagram for the same DC bias conditions in the BJT and HBT. (c) Current gain β versus J_C in both structures.

To illustrate the characteristics of carrier transport inside the devices, Fig. 3 depicts the 2D electric field in the HBT for low and high V_{BE}. Moreover, Fig. 4(a) shows the average carrier concentration in the HBT for two bias conditions. Fig. 4(b) reports the comparison of the electron energy under high-injection conditions in the BJT and HBT for identical J_C (equal to 530 A m^{-1}). Both, carrier concentration and energy are the vertical profiles calculated from the emitter electrode to the collector. It can be observed how, at low J_C ($V_{BE} = 0.75$ V) in the HBT (Fig. 3(a)), the field in the collector–base (CB) region has the expected triangular shape with a negative maximum located close to the metallurgical junction (≈0.11 μm). Since the CB junction is under reverse bias conditions, any incident electron that reaches its edges is quickly swept across to the sub-collector by the high electric field. For *low-injection* conditions the electron density in the collector depletion region is significantly smaller than the background donor or acceptor density (Fig. 4(a)).

As V_{BE} increases, a deviation of J_C from the low-bias condition occurs in both transistors (Fig. 2(a)), its origin being governed by different factors. First, the *high-level injection* at the EB junction [9] takes place; its threshold condition occurs when the injected minority carrier concentration level in the neutral base increases reaching a value around 10% of the majority carrier concentration. This high-level threshold voltage, $V_{BE\text{-}hl}$, is equal to 0.92 V in the BJT and 0.83 V in the HBT, both close to the analytical calculation [9] (the conduction band lowering and the aiding quasi-electric field in the EB junction reduces $V_{BE\text{-}hl}$ in the HBT). In this regime, as a consequence of the high injection of electrons into the base, the majority carrier concentration (holes) also increases to maintain quasi-neutrality, as observed in Fig. 4(a). This effect makes J_C become proportional to $\exp(qV_{BE}/2K_BT)$ (Fig. 2) [10]. This is still a 1D effect which could be avoided in the HBT by increasing the base doping density. Since our purpose is to study the effect of the Ge content in the HBT base, the benefits induced in the HBT performance by the possibility of increasing the base doping density will not be analyzed.

When the collector current density is very high (as V_{BE} is further increased) the charge density of electrons

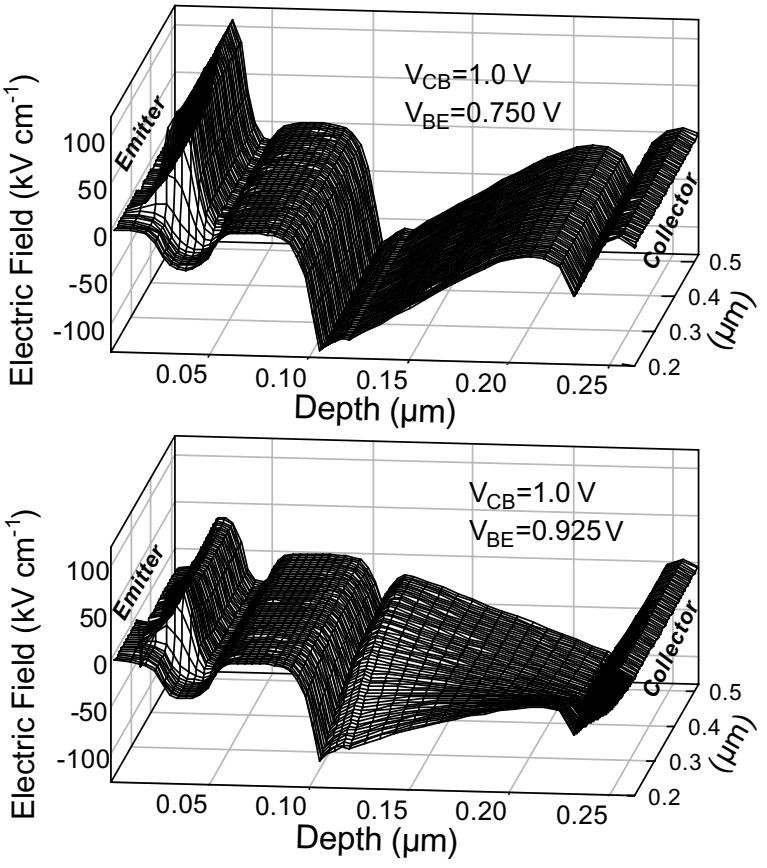

Fig. 3. Two-dimensional electric field in the HBT from the emitter to the collector (normal to the plane of the junctions) for low (0.750 V) and high (0.925 V) V_{BE}. For the sake of clarity the electric field is represented only under the emitter contact.

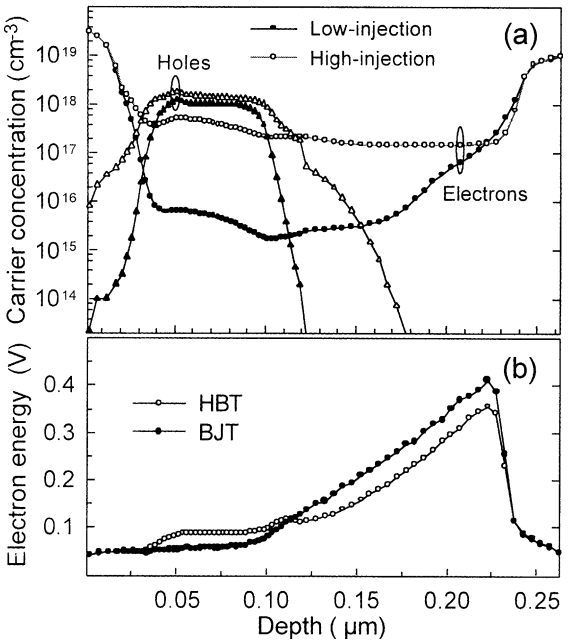

Fig. 4. (a) Electron and hole concentrations in the region localized under the emitter in the HBT under *low*-($J_C = 10\ A\,m^{-1}$, thin lines) and *high-injection* conditions ($J_C = 530\ A\,m^{-1}$, thick lines). (b) Energy profiles from the emitter to the collector in the BJT and HBT for $J_C = 530\ A\,m^{-1}$ in both structures corresponding to high-injection conditions.

in the CB space-charge layer may become comparable to the doping density on either one or both sides of the CB junction (Fig. 4(a)). This leads to the phenomenon called *push-out of the base* (or Kirk effect) [11]. The onset of this effect takes place for values of J_C around $136\ A\,m^{-1}$ in the BJT and $107\ A\,m^{-1}$ in the HBT. Many consequences arise from this effect and can be easily detected in the HBT by means of the comparison of the electric field under low and high applied V_{BE} (Fig. 3(a) and (b), respectively). First a widening of the quasi-neutral base, which penetrates into the collector. Second a 2D distortion of the electric field in the CB junction, which makes it exhibit a spatial dependence in the plane of the junctions. Moreover the highest field region suffers a displacement towards the sub-collector, where the doping is sufficiently large to allow the depletion region to form. The Kirk effect remains equally important in HBTs and BJTs [12]. These *high-injection* phenomena are largely responsible for the drop in the device performance (β or f_T fall off) at high J_C (Fig. 2(c)) and may have a strong influence on the noise behavior, as will be shown in next sections.

An estimation of f_T in both structures made by means of the quasi-static approach (or charge control principle) [13,14] gives values of 20 and 33 GHz in the Si BJT and SiGe HBT, respectively.

3.2. Autocorrelation functions and spectral densities

Fig. 5(a) and (b) shows C_{J_E}, C_{J_B}, and C_{J_C} and the cross-correlation functions, $C_{J_EJ_C}$, $C_{J_BJ_C}$, and $C_{J_EJ_B}$ in the BJT and in the HBT, respectively. The DC bias conditions of both structures correspond to a similar collector current density around $5.6\ A\,m^{-1}$. It may be seen that the autocorrelation functions of the emitter, base and collector current fluctuations are characterized by the typical exponential decay for short times and then all exhibit a negative part due to the coupling between the fluctuations of the electric field and carrier velocity [4].

Even if the typical frequency range of operation of bipolar transistors does not exceed 100–150 GHz, since our model can provide the noise at frequencies much higher than those experimentally attainable, we report the values of the spectral densities reaching the THz range to illustrate the physics of the processes controlling the noise at so high frequencies. The spectral densities are plotted in Fig. 6(a) and (b) for BJT and HBT, respectively, and for an identical collector current density as that of Fig. 5. The typical experimental noise spectra of these devices exhibit two main ranges as function of frequency. For frequency values lower than the $1/f$ corner frequency, f_C, the most important contribution is $1/f$ noise, while once the frequency surpasses f_C the noise spectra do not show significant frequency dependence (*white* noise). Our model excludes generation-recombination and other mechanisms responsible for $1/f$ noise, which determine the current spectral density in real devices at low frequencies. In the light of Fig. 6, the calculated low-frequency values of S_{J_i} and $S_{J_iJ_j}$ exhibit negligible frequency dependence up to values around 40 GHz, well above the disappearance of $1/f$ noise in the device. It can be observed that the term that

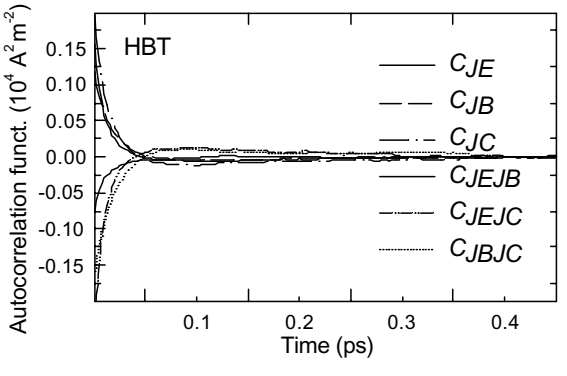

Fig. 5. The autocorrelation function of emitter, base and collector current fluctuations, C_{J_E}, C_{J_B} and C_{J_C} respectively (thick lines) together with the cross-correlation between pairs of these magnitudes $C_{J_EJ_C}$, $C_{J_BJ_C}$ and $C_{J_EJ_B}$ (thin lines) in the SiGe HBT for $J_C = 5.6\ A\,m^{-1}$.

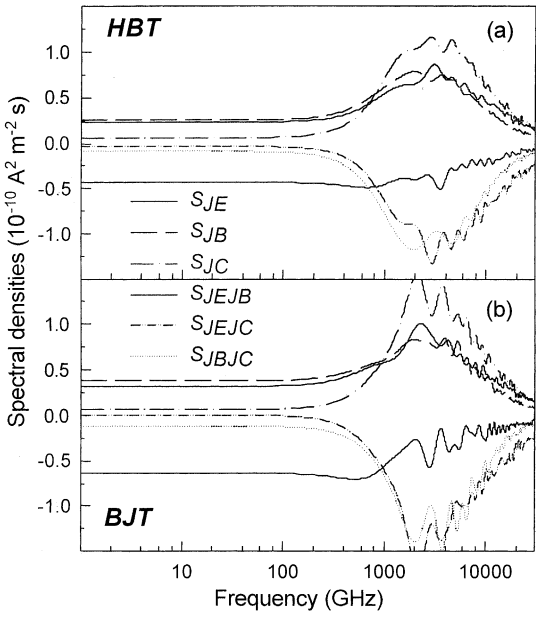

Fig. 6. Spectral densities of emitter, base and collector current fluctuations, S_{J_E}, S_{J_B}, S_{J_C} respectively (thick lines). Spectral densities of the cross-correlation between emitter and collector, base and collector, emitter and base current fluctuations, $S_{J_EJ_C}$, $S_{J_BJ_C}$ and $S_{J_EJ_B}$ respectively (hairlines) in (a) the Si BJT and (b) the SiGe HBT for $J_C = 5.6$ A m^{-1}.

exhibits a larger white noise range is $S_{J_EJ_B}$, which can be considered as frequency independent up to values around 200 GHz. On the contrary, the term that firstly begins to be influenced by frequency (around 40 GHz) is S_{J_C}. Therefore, it can be considered that our calculated low-frequency values $S_{J_i}(0)$ and $S_{J_iJ_j}(0)$ are RF values. Moreover, at very high frequencies, different maxima in S_{J_E}, S_{J_B} and S_{J_C} are detected, which are related to the oscillations of space charge at the plasma frequency in the highly doped regions [4,5,15].

For the DC condition considered here, when comparing the $S_{J_i}(0)$ and $S_{J_iJ_j}(0)$ terms of BJT and HBT (Fig. 6), the most significant noise reduction appears in the S_{J_B} and $S_{J_EJ_B}$ terms, 31% and 32%, respectively. This is due to the fact that for the same value of J_C, due to the introduction of Ge content a remarkable reduction of the base current (formed by holes crossing from the base towards the emitter) takes place in the HBT. Also, a lowering of 10% is found in $S_{J_EJ_C}$ and $S_{J_BJ_C}$ in the HBT (as compared to the BJT). In general, the differences reported here between the several noise terms depend on the bias conditions, as explained in next section.

3.3. Bias dependence of the RF spectral densities

The most frequently used noise models of BJTs and HBTs in the microwave frequency range are mainly developed on the basis of the pioneering work of van der Ziel [16] for BJTs. Different models derived from the noise theory of the BJT have been recently developed and proposed in the literature [17,18]. In general, the noise behavior of a linear noisy BJT or HBT can be accurately represented as a noiseless two-port circuit defined in terms of the Y-parameters combined with two noise current generators at the input and output, S_{J_B} and S_{J_C}, respectively. However, some of the noise sources usually included in the models are not very well known and typically they are assumed to be of thermal- or shot-noise type [17,18].

Our EMC simulation provides useful information about the above mentioned low-frequency values of $S_{J_B}(0)$ and $S_{J_C}(0)$ terms. Since their RF values are strongly related to the internal mechanisms controlling the device behavior (band discontinuities, injection level inside the devices, presence of hot carriers, etc.) [5,6], in this section we shall focus on their physical origin, paying special attention to the different injection conditions. As it has been stated in the previous section the calculated low-frequency values of S_{J_i} and $S_{J_iJ_j}$ are frequency independent (*white* noise) up to values around 40 GHz. Fig. 7 reports the comparison of the low-frequency plateau values $S_{J_B}(0)$ and $S_{J_C}(0)$ in the BJT and HBT as a function of J_C. We should remark that, due to the lack of statistical resolution in the presence of a high EB barrier, the Monte Carlo simulation is not able to provide reliable values of the current for values of V_{BE} lower than those reported in Fig. 2 and, for the same reason, the calculation of the noise becomes complicated (and less reliable) for the lowest values of J_C shown in Fig. 7.

Two well defined different regimes are observed in $S_{J_B}(0)$ (Fig. 7, circles). In our Monte Carlo simulation $S_{J_B}(0)$ is given mainly by the fluctuations related to the dynamics of holes in their movement from the base towards the emitter. First, for J_C lower than 20 A m^{-1} (low-injection level), we notice that $S_{J_B}(0)$ exhibits a slight variation with the DC point in both structures. This noise source located at the base terminal does not exhibit a pure shot-noise behavior ($2qJ_B$). This is due to the fact that the main contribution to the noise detected at the input comes from thermal component related to the base resistance, r_B, which includes the 2D behavior of the base current [17]. We confirm that the presence of a heterojunction does not imply distinguishing aspects in the operation of the HBT under low-injection conditions [10]. The same conclusion was attained in a 1D study of Si/SiGe heterojunctions [19]. The resistance, r_B, that accounts for the ohmic drop in the base region is bias dependent due to the "current crowding effect" [10] taking lower values when J_C increases. Moreover, for the largest values of J_C, when the base push-out occurs, the increment of the effective base width causes a further reduction of r_B [10]. The moderate increase observed in $S_{J_B}(0)$ for high values of J_C could be ascribed to both effects.

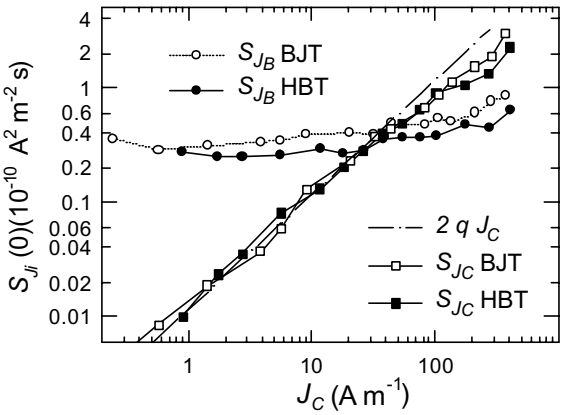

Fig. 7. Comparison of $S_{J_C}(0)$ and $S_{J_B}(0)$ in the Si BJT and SiGe HBT. $V_{CB} = 1.0$ V, J_C varies with V_{BE}.

In Fig. 7 it can also be observed how the injection conditions strongly govern the behavior of the $S_{J_C}(0)$ term. For the lowest J_C values (lower than 100 A m^{-1}), $S_{J_C}(0)$ suffers a pronounced increase with J_C, following a typical shot noise dependence ($2qJ_C$) in both structures, in agreement with that usually assumed in the literature [16–18]. However, while in circuit models this noise source is typically postulated to be constant and non-dependent on bias conditions, our results show that for J_C above 100 A m^{-1}, under high-injection conditions and when transport is no longer barrier-controlled, $S_{J_C}(0)$ deviates from the typical shot-noise response in both devices. This effect begins to occur at the current level for the onset of high-injection conditions and under the presence of hot carriers. In fact, once $S_{J_C}(0)$ leaves the shot-noise dependence, it tends to a flat thermal-like behavior for a very short J_C range and then it increases again with J_C due to the presence of hot carriers. This behavior is quite similar to that observed in other barrier-controlled devices like Schottky and pn diodes [5,15], but with a reduced thermal-noise range due to the complexity of the structure.

In fact, the displacement of the high-field BC region towards the sub-collector observed in Fig. 3 (Kirk effect) favors the appearance of hot carriers in a wide region of both structures (Fig. 4(b)) and yields the main differences between them. In SiGe HBTs once the push-out of the base is established, a low-field region (near to become a barrier) is formed at the original SiGe/Si hetero-interface [20] for the highest values of V_{BE} (Fig. 3(b)), which of course is absent in BJTs. The main consequence of the presence of this "barrier" is that it slightly reduces the appearance of hot carriers in the collector region of the HBT (and therefore their contribution to the excess noise) as compared with the BJT, leading to the differences observed in $S_{J_C}(0)$ between both devices (lower in the HBT) at the highest values of J_C. In contrast, the absence of a Ge grading and a SiGe base layer in the BJT avoids the heating of electrons when entering into the base, but leads to a linear increase of electron energy with position in their movement towards the sub-collector, reaching higher energy values than in the HBT over a wide collector region (Fig. 4(b)).

4. Conclusions

A comparative analysis of the noise behavior of a Si BJT and a Si-emitter/SiGe-base/Si-collector HBT with identical geometry and doping levels under different injection conditions has been realized by means of a 2D EMC simulator. The bias dependence of the noise sources typically used to characterize the noise in these devices by their inclusion in equivalent circuit models has been provided. The behavior of the noise sources is similar in both transistors. S_{J_B} is found to be mainly dominated by thermal noise related to the base resistance. This term does not show shot-noise behavior at any bias. In contrast, the S_{J_C} term behaves shot-noise like in a wide range of low and intermediate currents close to quasi-saturation, as usually assumed in circuit models. However, for the highest voltages, under high-injection conditions and when the EB barrier no longer controls J_C in the transistors, a deviation of S_{J_C} from the shot-noise behavior due to the onset of hot carriers effects is found.

The main difference between both transistors comes from the presence of the double heterojunction in the HBT base which, as a consequence of the narrow gap of the SiGe base, allows this device to provide a given level of J_C requiring a much lower value of J_B than the BJT, thus exhibiting a reduction of RF current noise, mainly related to the S_{J_B} term. Also other difference appears between both devices, mainly under or near high-injection conditions, when the effects related to the presence of the heterojunction become more evident in the noise of the devices. Thus, the quasi-electric field generated by the trapezoidal Ge profile at the EB junction and the barrier generated by the heterojunction at the CB SCR once the push-out of the base has taken place, have some effect on the S_{J_C} term, mainly regulating the importance of hot carrier effects on the noise in the transistors.

Acknowledgements

This work has been funded by Research Project PB97-1331 from the Dirección General de Enseñanza Superior e Investigación Científica and Research Project SA44/99 from the Junta de Castilla y León.

References

[1] Cressler JD. IEEE Trans Microwave Theory Tech 1998;46:572–89.
[2] Dodo H, Amamiya Y, Niwa T, Mamada M, Tanaka S, Shimawaki H. Proc IEEE MTT-S Int Microwave Symp Digs 1998;2:693–5.
[3] Jacoboni C, Lugli P. The Monte Carlo method for semiconductor device simulation. Vienna: Springer; 1989.
[4] Martín MJ, Pardo D, Velázquez JE. J Appl Phys 1998; 84:5012–20.
[5] Martín MJ, Pardo D, Velázquez JE. J Appl Phys 1996;79:6975–81.
[6] Peter MS, Klootwijk JH, Slotboom JW, van Rijs F, Terpstra D, De Boer WD. Proc of 29th European Solid State Device Conference, ESSDERC'99, Leuven, Belgium, September 1999, p. 716–20.
[7] Babiker S, Asenov A, Cameron N, Beaumont SP, Barker JR. IEEE Trans Electron Dev 1998;45:1644–52.
[8] Crabbé EF, Cressler JD, Pattyon GL, Stork JMC, Comfort JH, Sun YYC. IEEE Electron Dev Lett 1993;14: 193–5.
[9] Sah CT. Fundamentals of solid state electronics. Singapore: World Scientific; 1991.
[10] Muller RS, Kamins TI. Device electronics for integrated circuits. New York: Wiley; 1986.
[11] Kirk CT. IEEE Trans Electron Dev 1964;9:163.
[12] Tiwari S. Compound semiconductor device physics. Boston: Academic Press; 1992.
[13] Guillermo González G. Microwave transistor amplifiers. New Jersey: Prentice Hall; 1997.
[14] Hueting RJE. Charge carrier transport in silicon-germanium heterojunction bipolar transistors. Veenendall: Universal Press; 1997.
[15] Varani L, Reggiani L, Kuhn T, González T, Pardo D. IEEE Trans Electron Dev 1994;41:1916–25.
[16] Ziel AVD. Proc Institute of Radio Engineers 1958; 46:1019–38.
[17] Rudoph M, Doerner R, Klapproth L, Haymann P. IEEE Electron Dev Lett 1999;20:24–6.
[18] Escotte L, Roux JP, Plana R, Graffeuil J, Gruhle A. IEEE Trans Electron Dev 1995;42:883–9.
[19] Martin MJ, Pardo D, Velazquez JE. Semicond Sci Technol 2000;15:277–85.
[20] Joseph AJ, Cressler JD, Richey DM, Niu G. IEEE Trans Electron Dev 1999;46:1347–54.